Pacific Graphics (2015)
N. J. Mitra, J. Stam, and K. Xu (Editors)

*Short Paper*

# Simultaneous Stereo Rectification and Distortion Correction with Application to DoF Synthesis

Chen Ting Yeh[1], Tien-Yu Ho[2], Szu-Hao Huang[3] and Shang-Hong Lai[1]

[1] Department of Computer Science, National Tsing Hua University, Taiwan
[2] Institute of Information Systems and Applications, National Tsing Hua University, Taiwan
[3] Department of Information Management and Finance, National Chiao Tung University, Taiwan

**Abstract**

*Stereo rectification based on epipolar geometry is an image transformation process which is used to align the rectified stereo images to be coplanar. For image pairs captured by low-cost stereo camera systems, image noises and optical distortions in images may lead to errors in depth estimation. In this paper, a novel algorithm is proposed to simultaneously solve the stereo rectification and distortion correction problems in an integrated optimization framework. The estimated disparity maps are then used to synthesize the depth of field (DoF), which is to increase the saliency of the foreground objects, with the proposed spatially-variant filtering method. Experimental results on various synthetic and real stereo images are shown to demonstrate that the proposed algorithm can effectively reduce the stereo rectification error by considering the optical distortion model. The DoF synthesis can also be improved by using more accurate disparity estimation results.*

## 1. Introduction

Stereo vision has been widely applied to geometric model reconstruction, robot vision, passive object scanning, and 3D display applications. In the 3D vision research, stereo rectification plays an important role to simplify the disparity estimation process. In addition, large amounts of stereoscopic images and videos are available on public domain due to the popularization of low-cost stereo camera systems. However, the images captured by low-cost stereo cameras might have several optical defects, such as defocus, high noises, and optical distortion. In this paper, we propose a novel algorithm for simultaneous stereo rectification and distortion correction to improve the accuracy of disparity estimation from uncalibrated stereo images. Then, we demonstrate that the estimated depth information can be used to generate depth of field (DoF). With our algorithm, using low-cost stereo cameras can also generate photos with various DoF as DSLR camera does.

To estimate the disparity maps from stereo image pairs is a fundamental problem for most advanced 3D stereo applications. In order to improve the efficiency of disparity estimation, the image rectification is required to transform a pair of stereo images onto a common image plane by applying homography transformations based on the epipolar geometry. For related works on stereo rectification, Heller and Pajdla [HP09] proposed to map epipolar curves onto circles to rectify the stereo omnidirectional images. Geyer and Daniilidis [GD03] proposed a new algorithm for the rectification of two omnidirectional cameras. DoF and bokeh effect are image synthesis techniques to highlight the target object and blur the background regions. The issue is also well-known as the shallow DoF of DSLR camera. McGraw, T. [McG14] proposed a method for rendering bokeh effects using low-rank linear filters. Their technique can simulate lens spherical aberration which causes nonuniform bokeh intensity. Moersch, J. et al. [MH14] presented the Flexible Linear-time Area Gather (FLAG) blur algorithm with a variable-sized circular bokeh for producing DoF on rasterized images.

In this paper, a new stereo rectification method is proposed. The images captured by the principal camera are the reference images which are assumed to contain very small distortion effect, and the images captured by the secondary camera should be corrected by the estimated distortion parameters. The main idea of this research is to model the parameters of distortion effect and stereo rectification process into an integrated energy function, then a global optimal solution is found to solve these two problems simultaneously. An accurate stereo rectification algorithm is proposed to im-



DOI: 10.2312/pg.20151280

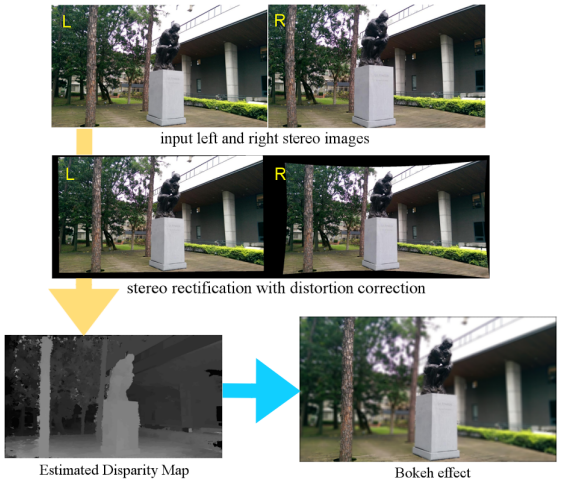


**Figure 1:** *Demonstration of the proposed stereo rectification with distortion correction and synthetic DoF*

prove the accuracy of depth estimation. The precise depth information can be applied to synthesize the DoF effect. Figure 1 shows an example processing flow of the proposed system, including input stereo images, rectification results with distortion correction, depth estimation, and DoF synthesis. The experimental results show that the proposed system can achieve better rectification results under various distortion conditions and generate the photos with DoF under various DoF settings.

## 2. Stereo Rectification with Distortion Correction

This section reviews two well-developed algorithms, stereo rectification [FI08, IT99] and radial distortion model [BD05], and proposes a new intergrated framework.

### 2.1. Uncalibrated Stereo Rectification

The goal of stereo rectification is to find the rectification homography matrices for the input stereo images. Extracting the discriminant feature points from each image and matching point pairs from stereo images is essential for 3D reconstruction from uncalibrated stereo cameras.

The estimated homography matrix $H$ can transform an image from the original projection matrix $P_o$ to a new one, $P_n$, based on the equation $P_n = HP_o$. The projection matrix $P_n$ is used to define a virtual camera system that aligns the epipolar lines to horizontal scan-lines. The projection matrix can be represented as $P = K[R|t]$, where $K, R$ and $t$ denote the calibration matrix, rotation matrix and translation vector, respectively. The rectification homography matrix can be written as:

$$H = P_{n1:3}P_{o1:3}^{-1} = K_n R_n R_o^{-1} K_o^{-1} = K_n R' K_o^{-1} \quad (1)$$

where the notation $P_{n1:3}$ and $P_{o1:3}$ means the first three columns of the matrix $P_n$ and $P_o$, respectively. $R'$ can be calculated from two rotation matrices by $R' = R_n R_o^{-1}$. Based on the two-view geometry, all corresponding points from the left and right images, denoted by $p_l$ and $p_r$, should satisfy the epipolar constraint, i.e. $p_r^T F p_l = 0$, where $F$ is fundamental matrix. The associated fundamental matrix after the image rectification should be a skew-symmetric matrix which is the cross-product matrix of the vector $e_1 = [1,0,0]^T$. Therefore, the rectified coordinates of the corresponding points $p_l, p_r$ in the two views after the associated homography transformations $H_l, H_r$ should satisfy the following epipolar geometry:

$$(H_r p_r)^T [e_1]_\times (H_l p_l) = (H_r p_r)^T \begin{bmatrix} 0 & 0 & 0 \\ 0 & 0 & -1 \\ 0 & 1 & 0 \end{bmatrix} (H_l p_l) = 0 \quad (2)$$

Finally, the fundamental matrix $F$ between the original image pairs can be represented by the following equation:

$$F = H_r^T [e_1]_\times H_l = K_{or}^{-T} R_r'^T K_{nr}^T [e_1]_\times K_{nl} R_l' K_{ol}^{-1} \quad (3)$$

### 2.2. Radial Distortion Model

The visual quality of synthesized images in 3D display applications highly depends on the quality of the depth information which relies on robust and accurate stereo rectification results. The rectification error will be increased with the increase of optical defects, such as radial distortion. For radial lens distortion in wide-angle and catadioptric lenses, Claus and Fitzgibbon [CF05] presented a new rational function (RF) model. Some researches about handeling radial distortion are also presented in [RF11,BD05]. The division model is proven to be useful for distortion correction in most computer vision applications. With one control parameter $\lambda$, the division model can transform the coordinate system as the following equation:

$$p_u = \frac{1}{1+\lambda r^2} p_d \quad (4)$$

where $r^2 = x_d^2 + y_d^2$, and $x_d, y_d$ are the horizontal and vertical distance from the image center, and $p_u$ and $p_d$ denote the undistorted and distorted coordinates, respectively.

A lift technique can be applied to simplify the nonlinear problem into a linear form by embedding the problem to a higher dimensional space [BD05]. Each distorted point in homogeneous coordinates $p_d$ can be mapped to $\tilde{p_d}$. We denote this lift operation as $\tilde{p_d} = \kappa(p_d)$ which also normalizes the coordinates by $K^{-1}$ simultaneously. The distortion correction process for the division model can be further expressed as a linear relationship in this lifted space. The undistorted coordinates can be computed with simple matrix

multiplication with the undistortion matrix $A$:

$$p_u = \begin{bmatrix} x_u \\ y_u \\ 1 \end{bmatrix} \sim \begin{bmatrix} x_d \\ y_d \\ 1+\lambda r^2 \end{bmatrix} = A\tilde{p_d} = \begin{bmatrix} 1 & 0 & 0 & 0 \\ 0 & 1 & 0 & 0 \\ 0 & 0 & 1 & \lambda \end{bmatrix} \begin{bmatrix} x_d \\ y_d \\ 1 \\ r^2 \end{bmatrix} \tag{5}$$

In addition to the coordinate system transformation, this matrix also can be applied to the $4 \times 4$ radial fundamental matrix $\tilde{F}$ and $3 \times 4$ radial homography matrix $\tilde{H}$ as follows:

$$p_{ur}^T F p_{ul} = \tilde{p_{dr}}^T A_r^T F A_l \tilde{p_{dl}} = \tilde{p_{dr}}^T \tilde{F} \tilde{p_{dl}} = 0 \tag{6}$$

### 2.3. Radial Fundamental Matrix

Traditional rectification assumes that the input stereo images come from identical or homogeneous camera system. For the uncalibrated and low-cost camera, the lens distortion is a critical issue which may decrease the accuracy of fundamental matrix estimation. In this paper, we propose a novel algorithm for simultaneous stereo rectification and radial distortion correction in an integrated framework.

Given a stereo image pair $I_l$ and $I_r$, captured from multi-resolution stereoscopic system with unknown calibration matrices ($K_l$ and $K_r$) and radial distortion parameters ($\lambda_l$ and $\lambda_r$). The correspondences $(p_{dl}, p_{dr})$ in the distorted coordinate space can be extracted by feature extraction and point matching algorithms. These points are first normalized by $K$ and then embedded to a lifted world coordinates. The pairs of matched points are expected to satisfy the radial fundamental matrix $\tilde{F}$ as equation (6). Note that the radial fundamental matrix is composed of $3 \times 3$ fundamental matrix $F$ and two independent undistortion matrices $A_l$ and $A_r$ for both sides, respectively. The epipolar geometry under radial distortion can be viewed as the following constraint equation in an optimization framework.

$$\tilde{p_{dr}}^T \tilde{F} \tilde{p_{dl}} = \kappa(p_{dr})^T A_r^T R_r'^T [e_1]_\times R_l A_l \kappa(p_{dl}) = 0 \tag{7}$$

Following the conclusion of the previous work [CF05], the new intrinsic parameters in the camera calibration matrices $K_{nl}$ and $K_{nr}$ can be set arbitrarily if vertical focal length and vertical coordinate of the principal point are the same. Different intrinsic parameter settings may lead to the same experimental results due to $K_{nr}^T [e_1]_\times K_{nl} \sim [e_1]_\times$. Hence, the matrices $K_{nl}$ and $K_{nr}$ can be ignored in parameter optimization.

## 3. Proposed System and Implementation

This section describes the proposed stereo rectification and DoF synthesis system. The major processes to estimate the depth information includes feature extraction and matching, outliers elimination and robust estimation, nonlinear optimization for radial homography, and image rectification with distortion correction. We summarize our system in Algorithm 1 and describe the system implementation details in this section.

**Algorithm 1** Rectification with Distortion Correction

**function** RECTIFYUNDIST($I_l, I_r$)
  feature extration and matching by SIFT [Low99] to generate $p_{dl}, p_{dr}$
  RANSAC [FB81] to prune outliers roughly with larger distance threshold(to tolerant inliers violate epipolar constraint due to radial distortion)
  $\theta_{lx} \leftarrow 0$ to reduce rectification distortion
  initialize $\phi = \{f_l, f_r, \theta_{ly}, \theta_{lz}, \theta_{rx}, \theta ry, \theta rz, \lambda_l, \lambda_r\}$ as $f = w + h; \theta = \lambda = 0;$
  optimization for $\phi* = argmin$ COST$(p_{dl}, p_{dr}, \phi)$
  calculate $K_{ol}, K_{or}, R_l, R_r, A_l, A_r$ from $\phi*$
  calculate new camera matrix $K_{nl}$ and $K_{nr}$ (eq.9)
  $\tilde{H} = K_n R A$ for both sides
  **return** $\tilde{H_l}, \tilde{H_r}$
**end function**

**function** COST($p_{dl}, p_{dr}, \phi$)
  calculate $K_{ol}, K_{or}, R_l, R_r, A_l, A_r$
  calculate Radial Fundamental Matrix $\tilde{F}$ (eq3,6)
  lift coordinates by $\kappa$ (eq.5)
  calculate cost(eq.7) for each pair of $\tilde{p_{dl}}, \tilde{p_{dr}}$
  add soft constraint by $\theta_x, \theta_y, \theta_z$
  **return** $\rho_s(E_{samp})$ see eq.(8)
**end function**

### 3.1. Nonlinear Parameter Optimization

Because equation (7) describes an algebraic error, the Sampson error [HZ03], which is the first-order approximation of geometric error, is introduced for nonlinear parameter optimization. The squared Sampson error for the $j$-th corresponding points can be defined as:

$$E_{samp} = \frac{\tilde{p_{dr}}^{jT} \tilde{F} \tilde{p_{dl}}^j}{(\tilde{F}\tilde{p_{dl}}^j)_1^2 + (\tilde{F}\tilde{p_{dl}}^j)_2^2 + (\tilde{p_{dr}}^{jT}\tilde{F})_1^2 + (\tilde{p_{dr}}^{jT}\tilde{F})_2^2} \tag{8}$$

The intrinsic camera model only contains one variable, focal length $f$. In the optimization procedure, the focal length is set to $w + h$ as the initial guess, where $w$ and $h$ are the image width and height, respectively. The unknown rotation matrices are controlled by the Euler angles $\theta_x, \theta_y$ and $\theta_z$, with respect to $x, y$ and $z$ axis, respectively, which are initially set to zero. The distortion parameters $\lambda$'s are also assumed to be zero as the initial setting in the nonlinear parameter optimization.

We minimize the sum of the robust Sampson errors, denoted by $\rho_s(E_{samp}(f_l, f_r, \theta_{yl}, \theta_{zl}, \theta_{xr}, \theta_{yr}, \theta_{zr}, \lambda_l, \lambda_r))$, to find the solution for the 9 parameters by using the Levenberg-Marquardt optimization algorithm. The Lorentzion (or Cauchy) robust error function $\rho_s(r) = log(1 + r^2/2\hat{\sigma}^2)$ is employed to alleviate the influence of outliers; the robust standard deviation $\hat{\sigma}$ is self-determined by the order statistics methods [BHS99]. Note that $\theta_{xl}$ is constantly set to zero and not included into the optimization process based on the

consideration of preserving maximal mapped image area as well as reducing perspective distortion and solution ambiguity, since the rectified images can be rotated along x-axis and still kept rectified. Moreover, we include additional soft constraints on the parameters into the cost function to reduce the ambiguity in the solution space based on the two assumptions: (1) the higer resolution side is expected to contain less radial distorion and (2) the stereo rectification prefers less rotation angles.

In general, adequate overlapped regions between stereo images is required for the stereo rectification. The rotation angles and translation between stereo cameras should be constrained. Thus, a regularity term is applied as the soft constraint to prevent large amount of the rotation angles.

### 3.2. Radial Homography Matrix Estimation

Then, the virtual camera matrix $K_n$ should be estimated for the homography matrix calculation which is used in stereo rectification. From the estimated camera-dependent focal length parameters, $f_l$ and $f_r$, the smaller one is selected as the $f_{min}$ to simultaneously keep the visual quality and solve the resolution degradation problem during the image rectification. A new calibration matrix can be derived as follows:

$$K_n = \begin{bmatrix} f_{min} & 0 & -x_0 + t \\ 0 & f_{min} & -y_0 \\ 0 & 0 & 1 \end{bmatrix} \tag{9}$$

where $[x_0, y_0, 1]^T \sim \hat{K_{nl}} R_l' K_{ol} [0,0,1]^T$ and the horizontal shift $t$ is introduced to model the disparity between right and left rectified images. The radial homography matrix, which combines perspective rectification and radial distortion correction, can also be rewritten from equation(1) to the following form:

$$\tilde{H} = HA = K_n R' K_o^{-1} A \tag{10}$$

### 3.3. Disparity Estimation and DoF Synthesis

The estimated radial homography matrix will be applied to transform the input stereo image pair to be coplanar, so that the computational complexity of disparity map estimation can be simplfied. The proposed system employs a well-known method, non-local cost aggregation stereo matching algorithm [Yan12], to generate the required depth map. With various image pre-processing steps such as image denoising and resizing, this algorithm can minimize the Census Transform cost [ZW94], which is robust to the illumination changes and color tone variations, of each horizontal lines. These improvements can achieve more accurate disparity estimation and generate a precise depth map, which will be used for the DoF synthesis.

In this paper, a user interactive image refocusing system is developed by using the estimated depth information. Multiple representative depth layers are first extracted directly from the input disparity map. The user should define the foreground region of original image with a click user interaction on image coordinate $(x_r, y_r)$. For each pixel in the processing image, the proposed system will calculate the specific blur function by the depth difference between the target pixel and selected reference pixel. The larger depth difference would lead to more serious blur effect in the proposed DoF synthesis algorithm. And the image regions in the same depth layer as the reference point will maintain the original intensity value. The image filter for the spatially-variant blur synthesis is given in the following equation:

$$\hat{I}(x,y) = \frac{\sum_{\Delta x^2+\Delta y^2 \le R^2} G_{x,y}(\Delta x, \Delta y) \cdot I(x-\Delta x, y-\Delta y)}{\sum_{\Delta x^2+\Delta y^2 \le R^2} G_{x,y}(\Delta x, \Delta y)} \tag{11}$$

$$G_{x,y}(\Delta x, \Delta y) = \frac{e^{-(\Delta x^2+\Delta y^2)/2|D(x,y)-D(x_r,y_r)|^2}}{2\pi |D(x,y)-D(x_r,y_r)|^2} \tag{12}$$

where $I(x,y)$ denotes the intensity value of pixel $(x,y)$, and $D(x,y)$ is the depth value of the pixel $(x,y)$, and the coordinate $(x+\Delta x, y+\Delta y)$ means a neighbor pixel of $(x,y)$ with shift $\Delta x$ and $\Delta y$ in the image plane. Besides, $R$ is a predefined distance to decide the size of the 2D convolution region.

## 4. Experiments

In this section, various experiments are introduced to demonstrate the proposed DoF synthesis system and stereo rectification framework with radial distortion correlation. Most of the numerical evaluation of stereo rectification is measured by the rectification error.

### 4.1. Experiments on Real Images

In this section, the experiments on the real testing images are performed to verify the proposed stereo rectification algorithm. Most of the stereo datasets from the public domain are captured by the professional camera and further processed with the camera calibration and image rectification methods. In this work, we collect more than 50 sets of stereo images with distortion effects for the evaluation. Figure 2 depicts an example of input stereo images in our dataset and the final rectified images by using the proposed algorithm. These two stereo input images may have different focal length, different field of view, and different distortion effects. The distortion effects can be easily observed from the distorted straight lines like the brown street lamp in left side, and the output images are well-aligned, which can be observed from the auxiliary horizontal lines.

Figure 3 uses the estimated radial distortion parameters to correct the input distorted image. It is obvious that the straight lines of the building or surface marking can be recovered effectively. From the borders of the resulting images, we can also find that the parameters of the division

**Figure 2:** *Example of rectification on real stereo images: the input stereo images (first row) and rectified images with auxiliary lines (second row).*

(a) (b)

**Figure 3:** *Image restoration with estimated radial distortion parameters: include (a)original input images and (b)the distortion correction results*

model are estimated accurately and the radial distortion is corrected by the proposed system.

The performance of the proposed stereo rectification system is evaluated by the accuracy of estimated distortion parameters and the vertical distance between the matched points in the rectified image pairs. The vertical distance can be calculated from the equation: $\left|(H_l x_l)_2^T - (H_r x_r)_2^T\right|$.

### 4.2. Numerical evaluation and comparisons

In this section, a series of numerical evaluation and comparisons are described. For each testing image, we compare the proposed system with other methods. An automatic distortion correction algorithm, Lee [LCL*11], and two well-known rectification methods, Hartley [Har99] and Fusiello [FI08], are also adopted in the numerical evaluations. Table 1 shows that the proposed system outperforms two-step methods in terms of rectification error after compensating the differences in focal length and radial distortion. Applying the distortion correction model [LCL*11] before the traditional rectification methods, these two-step approaches may overfit the point correspondences and generate large perspective distortion in the rectified results.

**Table 1:** *Numerical evaluation and comparisons.*

| Method | mean error | max error |
|---|---|---|
| proposed | 0.458 | 1.11 |
| Lee [LCL*11]+Hartley [Har99] | 0.96 | 5.16 |
| Lee [LCL*11]+Fusiello [FI08] | 3.302 | 19.12 |

### 4.3. Synthetic depth of field effect

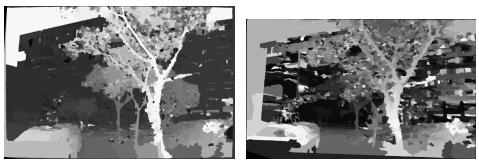

(a) proposed (b) Hartley [Har99]

**Figure 4:** *Estimated disparity maps by applying the stereo matching algorithm [Yan12] to the rectified stereo images by (a) the proposed method and (b) Hartley's method [Har99].*

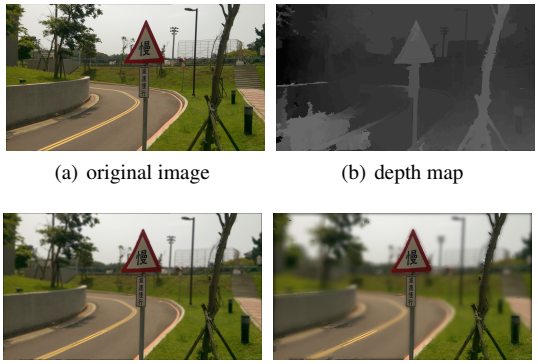

(a) original image (b) depth map

(c) slight DoF (d) obvious DoF

**Figure 5:** *DoF with different parameter settings*

The main application of stereo rectification is to reduce the computational complexity of stereo matching process. In this section, the rectified image results of the proposed system are used as the input images of Yang's [Yan12] non-local aggregation stereo matching algorithm for disparity estimation. Figure 4(a) shows that the higher quality of stereo rectification results by the proposed algorithm can improve the depth estimation accuracy dramatically. In contrast, the disparity map estimated from the rectified images by using Fusiello's method [FI08], shown in figure 4(b), is much more noisy and inaccurate.

Based on the depth information in the estimated disparity maps, the DoF is synthesized from the testing images with the spatially-variant filtering technique. A natural image, such as Fig 5(a), and its corresponding depth map, such as fig 5(b), are required for the proposed DoF synthesis system as the input data. In this example, the depth pixels are roughly clustered into four major depth groups before the image synthesis. And the user defines the traffic sign as their focus region. The remaining images in Figure 5 show the experimental results with different DoF levels, includes (c) slight effect and (d) obvious effect. Due to the similar depth values of the traffic sign and the tree at the right side of the image, the proposed system grouped them together to be in the same layer. Both of the objects are clear since user click on the traffic sign.

From the experimental results and analysis in this section, we can see that the performance of proposed DoF synthesis system may highly depend on the accuracy of depth estimation. This conclusion also points out that the improvement of stereo rectification and disparity estimation is very important and valuable for practical applications.

## 5. Conclusion

In this paper, a novel image rectification algorithm with radial distortion correction was proposed for uncalibrated stereo camera system. The nonlinear optimization method with soft constraints is applied to solve these two critical problems simultaneously. Based on the estimated depth information, a spatially-variant filtering method is proposed to synthesize the DoF. We demonstrate the proposed method with several experiments on real stereo images. Compared with the previous works, our method can achieve more accurate rectification results in the experimental comparisons and improve the visual quality of the synthesized DoF images.

For the future works, the rectification accuracy may be further improved by more complicated distortion model than the simple division model used in this paper. An integrated framework with global optimization may achieve better performance than the step-by-step system. Furthermore, in order to extend related researches to real-time applications, to implement the proposed system in the parallel computing platform, such as CUDA and HSA system, may increase the computational efficiency dramatically.

## Acknowledgements

This work was supported by Qualcomm Technologies, Inc.

## References

[BD05] BARRETO J. P., DANIILIDIS K.: Fundamental matrix for cameras with radial distortion. In *Computer Vision, 2005. ICCV 2005. Tenth IEEE International Conference on* (2005), vol. 1, IEEE, pp. 625–632. 2

[BHS99] BAB-HADIASHAR A., SUTER D.: Robust segmentation of visual data using ranked unbiased scale estimate. *Robotica 17*, 06 (1999), 649–660. 3

[CF05] CLAUS D., FITZGIBBON A. W.: A rational function lens distortion model for general cameras. In *Computer Vision and Pattern Recognition, 2005. CVPR 2005. IEEE Computer Society Conference on* (2005), vol. 1, IEEE, pp. 213–219. 2, 3

[FB81] FISCHLER M. A., BOLLES R. C.: Random sample consensus: a paradigm for model fitting with applications to image analysis and automated cartography. *Communications of the ACM 24*, 6 (1981), 381–395. 3

[FI08] FUSIELLO A., IRSARA L.: Quasi-euclidean uncalibrated epipolar rectification. In *Pattern Recognition, 2008. ICPR 2008. 19th International Conference on* (2008), IEEE, pp. 1–4. 2, 5

[GD03] GEYER C., DANIILIDIS K.: Conformal rectification of omnidirectional stereo pairs. In *Computer Vision and Pattern Recognition Workshop, 2003. CVPRW'03. Conference on* (2003), vol. 7, IEEE, pp. 73–73. 1

[Har99] HARTLEY R. I.: Theory and practice of projective rectification. *International Journal of Computer Vision 35*, 2 (1999), 115–127. 5

[HP09] HELLER J., PAJDLA T.: Stereographic rectification of omnidirectional stereo pairs. In *Computer Vision and Pattern Recognition, 2009. CVPR 2009. IEEE Conference on* (2009), IEEE, pp. 1414–1421. 1

[HZ03] HARTLEY R., ZISSERMAN A.: *Multiple view geometry in computer vision*. Cambridge university press, 2003. 3

[IT99] ISGRO F., TRUCCO E.: Projective rectification without epipolar geometry. In *Computer Vision and Pattern Recognition, 1999. IEEE Computer Society Conference on.* (1999), vol. 1, IEEE. 2

[LCL*11] LEE T.-Y., CHANG T.-S., LAI S.-H., LIU K.-C., WU H.-S.: Wide-angle distortion correction by hough transform and gradient estimation. In *Visual Communications and Image Processing (VCIP), 2011 IEEE* (2011), IEEE, pp. 1–4. 5

[Low99] LOWE D. G.: Object recognition from local scale-invariant features. In *Computer vision, 1999. The proceedings of the seventh IEEE international conference on* (1999), vol. 2, Ieee, pp. 1150–1157. 3

[McG14] MCGRAW T.: Fast bokeh effects using low-rank linear filters. *The Visual Computer* (2014), 1–11. 1

[MH14] MOERSCH J., HAMILTON H. J.: Variable-sized, circular bokeh depth of field effects. In *Proceedings of the 2014 Graphics Interface Conference* (2014), Canadian Information Processing Society, pp. 103–107. 1

[RF11] RINGABY E., FORSSÉN P.-E.: Scan rectification for structured light range sensors with rolling shutters. In *Computer Vision (ICCV), 2011 IEEE International Conference on* (2011), IEEE, pp. 1575–1582. 2

[Yan12] YANG Q.: A non-local cost aggregation method for stereo matching. In *Computer Vision and Pattern Recognition (CVPR), 2012 IEEE Conference on* (2012), IEEE, pp. 1402–1409. 4, 5

[ZW94] ZABIH R., WOODFILL J.: Non-parametric local transforms for computing visual correspondence. In *Computer VisionqXECCV'94*. Springer, 1994, pp. 151–158. 4